An investigation on dysphotopsia of a sigma-edged intraocular lens

Zhishan Gao (高志山), Meimei Kong (孔梅梅), Xinhua Li (李新华), Lei Chen (陈 磊), and Rihong Zhu (朱日宏)

School of Optical Engineering, Nanjing University of Science and Technology, Nanjing 210094

Received November 4, 2005

A sigma-edged design of intraocular lens (IOL) is proposed to minimize the reflected glare images associated with the edge. The optimal sigma inverse edge is investigated when pupil diameter is 5.0 mm by the established Escudero-Sanz's wide angle model. The non-sequential ray tracing program of Zemax-EE (Zemax Development Corp., San Diego, USA) is used to investigate the sigma edge of reducing the potential for edge glare phenomena. The results show that sigma-edged design can significantly reduce the reflected glare intensity on retina if the angle of its inverse edge is taken from 20 to 70 degrees.

OCIS codes: 190.5890, 220.2740, 170.4460.

The implantation of an intraocular lens (IOL) is a successful method to treat patients who have cataract extraction. At present, some clinical reports suggest that patients with the implantation of IOL occasionally also notice excessive glare and halos around point sources of light. The excessive glare and halos, or unwanted light images, are termed dysphotopsia[1−3]. The dysphotopsia may be induced by reflections among surfaces and edges of an IOL. It can be divided into two types of symptoms, positive and negative[1,2], and is relative to the type[3], material[2,4,5] and edge design[6−12] of an IOL. The postoperative glare phenomena caused by the edges of an IOL design were investigated by many surgeons. Some simulations found that sharp-edged (or square-edged) design could cause permanent intractable glare that appeared to the patients as a thin crescent or partial ring, and round- edged design reduced the potential for edge glare phenomena[6,7]. However, further studies found that an IOL with sharp rectangular optic edges also significantly inhibited posterior capsule opacification (PCO)[8−11]. So an IOL with a round anterior edge and a sharp posterior edge (round-/sharp-edged design) was proposed for reducing edge glare and preventing PCO[12]. For the same purpose, the modification of an IOL consisting of the texturing square edge was made for impairing the edge glare[13].

A sigma-edged IOL is also a sharp-edged design, which has an inverse edge made up of two parts: the anterior inverse edge and posterior inverse edge, like a Greek character "$\sum$" (see Figs. 1(a)—(c)). The anterior inverse edge is expected to prevent the edge glare rays straight ahead to the retina. The tip of its inverse edge is manufactured with small radius of about 0.03 mm with a special tool. In Fig. 1, three angles of inverse edges for sigma-edged IOLs are given as 15°, 45°, and 85°, respectively. In this paper, we report the use of Zemax-EE optical design software (Zemax Development Corp., San Diego, USA) to investigate the sigma-edged design of reducing the potential for edge glare phenomena.

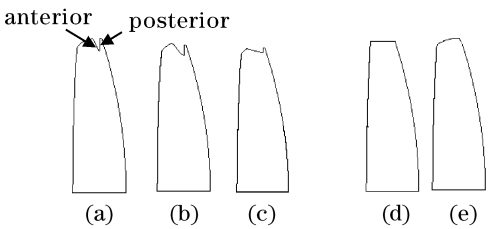

Fig. 1. Diagrams of three types of edge designs. (a)—(c) Sigma edges with different angles of inverse edge of 15°, 45°, 85°; (d) square edge; (e) round/sharp edge.

For analysis of the sigma-edged IOLs, we need to do two things: 1) setting up an experimental model of the pseudophakic eye with anatomical parameters; 2) using non-sequential ray tracing analysis to do computerized testing of the light pathways through IOLs.

Here the Escudero-Sanz's wide angle model is chosen as experimental model of the pseudophakic eye[14]. The two-dimensional (2D) layout of this model is shown in Fig. 2, where the anterior surface of cornea is aspherical, the posterior surface of cornea is spherical, and the stop surface (or iris) is placed in front of IOL. The retina of this model is defined as spherical surface. The coordinate system is depicted in Fig. 2, whose z axis is defined as the optical axis of the eye model and y axis inside the plane of paper. In order to emphasize the reflected glare intensity, we optimize the model eye including the

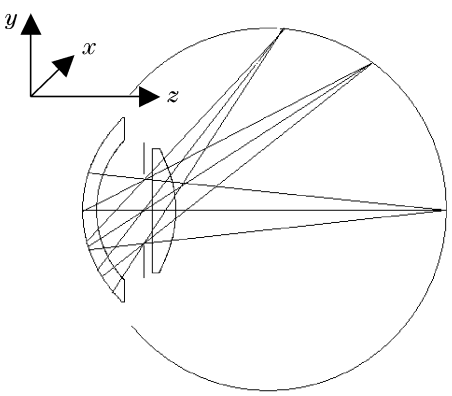

Fig. 2. Plot of the wide-angle eye model with a square-edged IOL.

Table 1. Prescription Data of the Pseudophakic Eye Model

Surface	Type	Radius (mm)	Thickness (mm)	Optical Medium	Conic Constant
1	Conic	7.72	0.55	Cornea	−0.26
2	Spherical	6.5	3.05	Aqueous	0
STO	Plane	∞	0.53	Aqueous	0
4	Spherical	194.93	0.9	Acrylic	0
5	Conic	−7.0	17.97	Vitreous	−2.1
Image	Spherical	−12.00			

investigated IOLs for minimizing the aberrations. The maximum field angle of this model eye is 60°. The prescription data are listed in Table 1. The simulation is carried out through a 5.0-mm pupil to simulate conditions of nighttime vision.

In order to obtain more general results, we address three types of IOLs with the same optic design (asymmetric biconvex, see Fig. 1): a square-edged design, a round-/sharp-edged design, and a sigma-edged design. Each IOL is of 5.5-mm clear diameter and made up of the acrylic. Its front surface is spherical with radius of curvature of 194.93 mm, and its rear surface is aspherical with apex radius of curvature of −7.0 mm and conic of −2.1. The central thickness is 0.9 mm.

The study is realized by using a glare source placed at 35° because it is demonstrated that this angle maximizes the intensity of the reflected image created by edge[6] and also to compare this analysis with others (carried out on difference lenses) that used this angle[12]. In addition, another glare ray tracing associated with the posterior inverse edge of a sigma-edged IOL needs to be considered, which is different from other IOL edge designs, because the posterior inverse edge can reflect rays from retina again to retina.

The further simulation is carried out to find the optimal sigma inverse edge. The relation between the angles of the sigma inverse edge and the associated retinal glare intensity are calculated by simulation.

In simulation, reflectivity at any boundary can be estimated by combining Fresnel's reflectivity equations and Snell's law to obtain[15],

$$R = \left(\frac{n_2 \cos\theta_2 - n_1 \cos\theta_1}{n_2 \cos\theta_2 + n_1 \cos\theta_1} \right)^2, \qquad (1)$$

where θ_1 is the angle of incidence and θ_2 is the angle of refraction. Although the sigma inverse edge may be rough and make the incidence rays scatter, for simplicity, its maximum reflectivity is also calculated according to Eq. (1).

For each edged-design IOL, we determine the patterns and intensity distributions of the reflected glare image at the curved retinal surface. For comparison, we define the intensity distributions of the reflected glare image on retina in terms of a relative intensity ratio. In the past, the results showed that an IOL with a round-/sharp-edged design produced the smallest intensity of the retinal glare image[12]. If the peak intensity of the reflected glare image on retina for the round-/sharp-edged design is $P_{\max}$, the relative intensity ratio is defined as $\frac{i_k(x,y)}{P_{\max}}$, where x and y represent coordinates on retina, $i_k(x,y)$ defines intensity distribution of the reflected retinal glare image, while the integer k is from one to three for the square-edged design, the round-/sharp-edged design, and the sigma-edged design, respectively.

Zemax-EE software reveals glare ray pathways reflected by edge as shown in Fig. 3, where the glare source is positioned at 35° from optical axis. Ray tracing shows two groups of rays: 1) rays that are refracted by anterior and posterior surfaces of the IOL to form the image of the glare source; 2) rays that are refracted by the anterior surface of the IOL, internally reflected by the edge of the IOL, and then refracted by posterior surface of the IOL, these rays form the reflected glare image on the retina opposite the glare image. In Figs. 3(a) and (b), some skew rays from a glare source at 35° are reflected internally towards the retina by square edge or the posterior square part of round/sharp edge. In Fig. 3(c), some skew rays from a glare source at 35° are reflected internally towards the cornea by the anterior inverse edge of a sigma-edged design, then reflected by anterior corneal surface (for this boundary is the interface of air and medium with refractive index of 1.3772, its reflectivity is much greater than others), and transmit through IOL to produce the reflected retinal glare image. From Figs. 3(a)—(c), we also find that only the minor rays near the brim of pupil form the retinal glare image associated with the IOL edge design.

The Zemax-EE software also finds another multi-reflection glare ray pathway associated with the posterior inverse edge of a sigma-edged design. The details of this glare ray pathway is shown in Fig. 4, where the rays transmit the eye model and focus on retina from a glare source positioned at angle from 5° to 10° near the optical axis, then are reflected by retina, finally reflected again by the posterior inverse edge of a sigma-edged design to retina.

Based on the above glare ray pathways associated with the edges of three types of IOLs, we can obtain the reflected glare intensity distributions on retina in terms

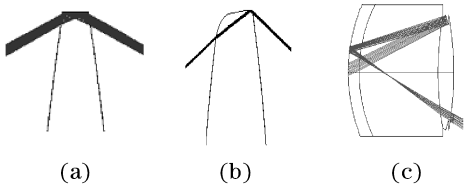

Fig. 3. Glare ray pathways reflected by the edges of three types of edge designs. (a) Square edge; (b) round/sharp edge; (c) sigma edge.

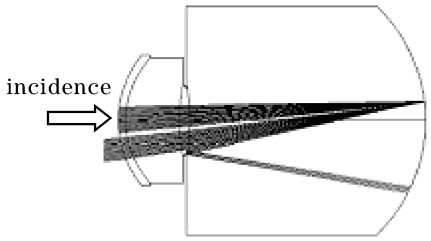

Fig. 4. Glare ray pathway associated with the posterior inverse edge of sigma-edged design.

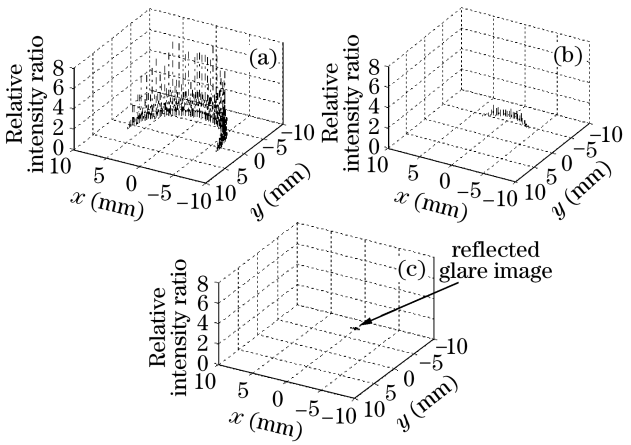

Fig. 5. Relative intensity ratio distributions of the reflected retinal images formed by the three types of edges. (a) Square-edged design; (b) round-/sharp-edged design; (c) the anterior edge of sigma-edged design.

of the relative intensity ratio. In this paper, all the simulations are done under the same conditions of the number of rays for ray tracing, the intensity distribution on pupil, and the size of pupil.

Figure 5 shows the relative intensity ratio distributions formed by ray reflection from the square-edged design, the round-/sharp-edged design, and the anterior edge of sigma-edged design. In Fig. 5, the vertical axis defines the relative intensity ratio, and the x and y coordinates define the location of the reflected glare image on retina. The origin ($x = 0$, $y = 0$) is the intersection of retina and the optical axis. From Fig. 5(b), we find the maximum relative intensity ratio of the reflected glare image by the round-/sharp-edged design is 1.0. The location of the reflected glare image is at point $(0, -5)$, under the origin and opposite the image of the glare source at 35°. The reflected glare image looks like a short partial ring (about 8 mm in length). From Fig. 5(a), we find the maximum intensity ratio of the reflected glare image by the square-edged design is much greater than that by round-/sharp-edged design. The corresponding reflected glare image looks like narrow half moon (about 15 mm in length). The location of its center is also at point $(0, -5)$. From Fig. 5(c), we find the maximum intensity ratio of the reflected glare image by sigma-edged design is only 0.1, i.e., much less than that by the round-/sharp-edged design. The corresponding reflected glare image is the shortest among the three types of edge designs. The location of its center is at point $(0, -8)$, farther from the origin than the other two types.

The angle of inverse edge of the sigma-edged design with the results in Fig. 5(c) is 15°. While it varies from small to large angle (about 5° to 85°), we simulate the reflected glare image again with the glare source point positioned at 35°. The relationship between the maximum relative intensity ratios of the glare image reflected by the anterior edge of a sigma-edged IOL and the angle of the inverse edge is shown in Fig. 6. From the figure, we find the relative intensity ratio increases between the angle range from 0° to 5° or from 75° to 85°. Especially, the maximum relative intensity ratio is near 8.0, similar to the results of Fig. 5(a). It is reasonable that the sigma-edged design with the angle near 90° tends to be the square-edged design. According to the results of Fig. 6, the optimal inverse edge should be with the angle greater than 20° and less than 70°. This optimal angle range for sigma-edged design should be further verified through the future clinical experiments.

The relative intensity ratios of the reflected retinal images formed by the posterior inverse edge (its reflected glare ray pathways shown as Fig. 4) are less than that by the anterior inverse edge of sigma-edged design. The corresponding results are shown in Fig. 7. As examples, the results of the reflected glare images for the angle of inverse edge with 15°, 25°, 35° and 45° are given. For simplicity, we suppose the reflectivity of retina about 75% at the wavelength of 0.5 μm[4].

The results obtained with the Zemax-EE software demonstrate that the rays reflected by the square-edged design can form an image with shape of narrow half moon or partial ring on the side of retina opposite the image of

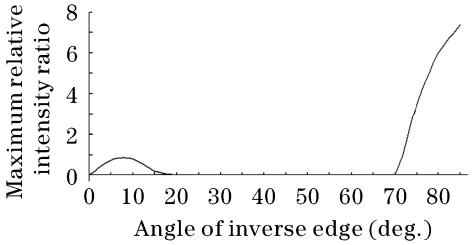

Fig. 6. Relationship between the relative intensity ratios of the glare image reflected by the anterior edge and the angle of the inverse edge.

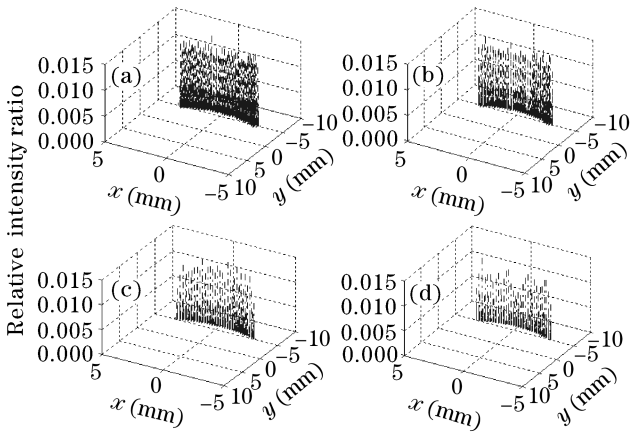

Fig. 7. Relative intensity ratio distributions of the retinal images formed by the posterior inverse edge of sigma-edged design. The angle of inverse edge of sigma-edged design is variable with 15° (a), 25° (b), 35° (c), and 45° (d).

the glare source. These results agree with those of Holladay *et al.*[6]. The results also demonstrate that the rays crossing the round-/sharp-edged design can reduce the intensity of the reflected image by a factor of 8.0 in comparison with the square-edged design, which agrees with those of Franchini *et al.*[12].

Our results also show the further decrease in the reflected glare with sigma-edged design in comparison with round-/sharp-edged design, while the angle of the inverse edge is from 20° to 70°. But when the angle of the inverse edge is larger than 75°, the relative intensity ratio of the reflected glare may be as strong as that of square-edged design. The reflected glare associated with the posterior inverse edge is another factor that may affect the visual image of patients, but it is less than those associated with the anterior inverse edge.

It is now necessary to determine whether the sigma-edged design corresponds to having the potential of weakening the reflected glare clinically. If this is the case, we will have an IOL with a sharp anterior edge that reduces the reflected glare on retina more effectively and with a sharp posterior edge that protects against the migration of lens epithelial cells across the poster capsule. This ensures the best quality of vision for the pseudophakic patients.

It needs to be noticed that the process of manufacturing a sigma-edged IOL has a bit of difficulty and needs to be discussed in the future. Especially the tips of inverse edge need to be manufactured with a special tool.

We thank Mr. Changzheng Huang, the president of Able Eye Device Ltd., for providing the samples of sigma-edged IOLs. Z. Gao's e-mail address is zhishgao@mail.njust.edu.cn.

References

1. J. Narváez, C. S. Banning, and R. D. Stulting, J. Cataract Refract. Surg. **31,** 846 (2005).
2. J. A. Davision, J. Cataract Refract. Surg. **26,** 1346 (2000).
3. R. Tester, N. L. Pace, M. Samore, and R. J. Olson, J. Cataract Refract. Surg. **26,** 810 (2000).
4. J. C. Erie, M. H. Bandhauer, and J. W. McLaren, J. Cataract Refract. Surg. **27,** 614 (2001).
5. J. C. Erie and M. H. Bandhauer, J. Cataract Refract. Surg. **29,** 336 (2003).
6. J. T. Holladay, A. Lang, and V. Portney, J. Cataract Refract. Surg. **25,** 748 (1999).
7. M. F. Ellis, J. Cataract Refract. Surg. **27,** 1061 (2001).
8. S. Masket, J. Cataract Refract. Surg. **26,** 145 (2000).
9. W. Buehl, O. Findl, R. Menapace, G. Rainer, S. Sacu, B. Kiss, V. Petternel, and M. Georgopoulos, J. Cataract Refract. Surg. **28,** 1105 (2002).
10. O. Nishi, K. Nishi, and K. Wickström, J. Cataract Refract. Surg. **26,** 1543 (2000).
11. O. Nishi and K. Nishi, J. Cataract Refract. Surg. **29,** 348 (2003).
12. A. Franchini, B. Z. Gallarati, and E. Vaccari, J. Cataract Refract. Surg. **29,** 342 (2003).
13. K. Hayashi and H. Hayashi, J. Cataract Refract. Surg. **30,** 1668 (2004).
14. I. Escudero-Sanz and R. Navarro, J. Opt. Soc. Am. A **16,** 1881 (1999).
15. D. Yu and H. Tan, *Engineering Optics* (in Chinese) (China Machine Press, Beijing, 2002) p.189.